Biology Contribution

Low Doses of Radiation Increase the Immunosuppressive Profile of Lung Macrophages During Viral Infection and Pneumonia

Lydia Meziani, PhD,[*,†] Charlotte Robert, PhD,[*,†,‡]
Marion Classe, MD, PhD,[*,§] Bruno Da Costa, Eng,[‖]
Michele Mondini, PhD,[*,†] Céline Clémenson, PhD,[*,†]
Alexia Alfaro, BEng,[¶] Pierre Mordant, MD, PhD,[#]
Samy Ammari, MD, MSc,[**,††] Ronan Le Goffic, PhD,[‖] and
Eric Deutsch, MD, PhD[*,†,‡]

*INSERM U1030, Molecular Radiation Therapy and Therapeutic Innovation, Gustave Roussy Cancer Campus, Université Paris-Saclay, Villejuif, France; †Labex LERMIT, DHU TORINO, SIRIC SOCRATE, Villejuif, France; ‡Department of Radiation Oncology, Gustave Roussy Cancer Campus, Villejuif, France; §Department of Pathology, Gustave Roussy Cancer Campus, Villejuif, France; ‖Université Paris-Saclay, INRAE, UVSQ, VIM, Jouy-en-Josas, France; ¶Gustave Roussy, Plateforme Imagerie et Cytométrie, UMS 23/3655, Université Paris-Saclay, Villejuif, France; #Department of Vascular Surgery, Thoracic Surgery, and Lung Transplantation, Bichat Hospital, Assistance Publique−Hôpitaux de Paris, INSERM U1152, Université de Paris, Paris, France; **Department of Radiology, Gustave Roussy Cancer Campus, Université Paris-Saclay, Villejuif, France; and ††BioMaps (UMR1281), Université Paris-Saclay, CNRS, INSERM, CEA, Orsay, 91471, France

Purpose: Severe pneumonia and acute respiratory distress syndrome (ARDS) have been described in patients with severe coronavirus disease 2019 (COVID-19). Recently, early clinical data reported the feasibility of low doses of radiation therapy (RT) in the treatment of ARDS in patients with severe COVID-19. However, the involved mechanisms remained unknown.
Methods and Materials: Here, we used airways-instilled lipopolysaccharide (LPS) and influenza virus (H1N1) as murine models of pneumonia, and toll-like receptor (TLR)-3 stimulation in human lung macrophages.

Results: Low doses of RT (0.5-1 Gray) decreased LPS-induced pneumonia, and increased the percentage of nerve- and airway-associated macrophages producing interleukin (IL) 10. During H1N1 viral infection, we observed decreased lung tissue damage and immune cell infiltration in irradiated animals. Low doses of RT increased IL-10 production by infiltrating immune cells into the lung. Irradiation of TLR-3 ligand-stimulated human lung macrophages ex vivo increased IL-10 secretion and decreased interferon γ production in the culture supernatant. The percentage of human lung macrophages producing IL-6 was also decreased.

Conclusions: Our data highlight a mechanism by which low doses of RT regulate lung inflammation and skew lung macrophages toward an anti-inflammatory profile. These data provide a preclinical mechanistic support to clinical trials evaluating low doses of RT, such as COVID-19-induced ARDS.

Introduction

The coronavirus disease 2019 (COVID-19) pandemic is responsible for more than 1.8 million deaths and 85.8 million cases worldwide as of January 5, 2021. The responsible agent, severe acute respiratory syndrome coronavirus 2 (SARS-CoV-2), is an enveloped RNA virus of the Coronaviridae virus family. Human-to-human transmission occurs through respiratory droplets or contaminated surfaces.[1] The average incubation period is 5 days, with a range of 1 to 14 days. Most patients present mild respiratory tract infections, most commonly characterized by fever (82%) and cough (81%). Severe pneumonia and acute respiratory distress syndrome (ARDS) have been described in 14% of the reported cases, and the overall mortality is around 1% to 2%.[2] Current therapeutic approaches involve mechanical ventilation, acute supportive care management of organ failure, steroids, and antiviral therapies such as remdesivir. Growing information suggests that patients with severe COVID-19 have a marked inflammatory state characterized by a cytokine storm syndrome similar to that seen in severe influenza cases,[3] and high levels of both calprotectin and myelopoiesis.[4]

Chest irradiation at a low dose has been used successfully in the past to treat pneumonia, especially before the onset of effective antimicrobial agents. The estimation of the radiation doses absorbed by the lungs is complex during orthovoltage irradiation techniques. Clinical reports suggest early improvement of breathing difficulties within hours and a reduction of mortality.[5-7] Currently, several clinical trials are underway (referenced on clinicaltrial.gov) and some studies, even if in small cohorts, have confirmed the efficacy of low doses of radiation therapy (RT) in the treatment of ARDS in patients with severe COVID-19.[8-11] However, the involved mechanisms remain unknown, and the use of chest RT for COVID-19 patients has been the subject of a vivid scientific controversy. Among the authors, the absence of proof of concept, as well as the intrinsic risk of radiation inducing lung damage and boosting viral expansion after RT, contribute to both for and against arguments.

RT exerts well-known anti-inflammatory properties when used at doses up to 1 Gray (Gy), while producing proinflammatory effects at higher doses,[12] highlighting the complexity of the immunologic mechanisms and the interrelationship between ionizing radiation (IR) and inflammation.

Pulmonary macrophages have been implicated in maintaining lung homeostasis by immune surveillance and clearance of dead cells, debris, and invading pathogens. The lung harbors 2 distinct populations of macrophages: alveolar macrophages (AMs) and interstitial macrophages (IMs).[13,14] AMs are located in alveolar space and seem to play a direct antiviral role, since AM depletion yields higher viral loads. IMs are located in the interstitium, along with dendritic cells and lymphocytes. Recently, a new IM subpopulation of nerve- and airway-associated macrophages (NAMs) has been characterized in mice.[15] NAMs are distinct from other lung-resident macrophage subsets, and highly express immunoregulatory genes. NAMs proliferate robustly after influenza infection and activation with the polyinosinic:polycytidylic acid [Poly(I:C)], and in their absence the inflammatory response is augmented, resulting in excessive production of inflammatory cytokines and innate immune cell infiltration. NAMs function to maintain immune and tissue homeostasis, and regulate infection-induced inflammation through the secretion of immunosuppressive factors such as interleukin (IL) 10. Viral infection in the absence of NAMs is associated with an excess of proinflammatory cytokines and chemokines such as IL-6, (C-C motif) ligand (CCL) 2, CCL3, and CCL5, eventually leading to massive lung damage and death.[15] Interestingly, potential pathologic roles of macrophages during SARS-CoV-2 infection have been described.[16]

Irradiation has a direct effect on macrophage activation, depending on the time, dose, and subpopulation. In the tumor stroma, high doses of IR (>8 Gy) promote anti-inflammatory activity of macrophages,[17] and low doses (<2 Gy), either alone or combined with immunotherapy, induce proinflammatory activity of macrophages.[18,19] Within the lung, irradiation at a high dose (16 Gy) affects the phenotypes of alveolar and interstitial macrophages differently, resulting in distinct local cytokine and chemokine microenvironments in the tissue and alveoli. Interestingly, there is a difference between lung subcompartments in response to a fibrogenic irradiation dose (16 Gy), with an immune response first in the parenchyma and then in the alveolar compartment.[20]

In the present study, using a lipopolysaccharide (LPS), influenza A PR8 virus (H1N1), or toll-like receptor 3 (TLR3) ligand Poly(I:C) as inductors of inflammation,[21] and low doses of RT as a potential treatment, we

investigated whether RT could be involved in counteracting lung inflammation through IL-10 production.

Methods and Materials

Human tissue samples

All patients signed an informed consent allowing the use of their surgical specimen for research purposes. The database was declared to the National Board for Informatics and Freedom (Commission Nationale Informatique et Liberté, CNIL, authorization #2217874) and to the National Institute for Health Data (Institut National des Données de Santé, INDS, authorization #MR4316030520). Immediately after anatomic lung resection for lung cancer (n = 3) or benign disease (n = 1), a 2-cm wide peripheral wedge of macroscopically normal lung parenchyma was harvested on the surgical specimen and kept in a sterile saline solution at 4°C.

Animals

Animal procedures were performed according to protocols approved by the Ethical Committee XXXX XX and in accordance with recommendations for the proper use and care of laboratory animals. For the pneumonia model, female C57BL/6 mice (10 weeks old) were purchased from Janvier Laboratories.

LPS and Poly(I:C) administration

For the pneumonia model, mice were anesthetized (isoflurane), and either LPS (O55:B5) or Poly(I:C) in 50-μl sterile phosphate-buffered saline (PBS) or PBS alone (for controls) was administered intratracheally. Mice received 2 sublethal doses of LPS (100 μg and 50 μg) or Poly(I:C) (100 μg and 50 μg), with a 24-hour rest period between each administration.

Influenza A virus instillation

Mice received a lethal dose (500 plaque-forming unit) of influenza virus (A/Puerto Rico/8/1934 [H1N1]) in 50 mL of PBS by intranasal instillation.

Irradiation procedure

At 6 hours after the second administration of LPS or Poly(I:C), the mice were immobilized by anesthesia (2% isoflurane) and locally irradiated at the thorax using a Varian Tube NDI 226 (X-ray machine; 250 kV; tube current, 15 mA; beam filter, 0.2 mm Cu), with a dose rate of 1.08 Gy•min−1. A single dose of 0.5 or 1 Gy was locally delivered to the whole thorax.

Dexamethasone administration

A single dose of 10 mg/kg of dexamethasone (Dexamethasone Mylan 4 mg/1ml, solution for injection, lot n°200147, Mylan) was administered to the mice by intraperitoneal injection.

Computed tomography imaging

Mice underwent computed tomography (CT) scans at the lung level. During scanning, mice were immobilized by anesthesia (2% isoflurane). ImageJ software was used to quantify lung density on axial slices.

Bronchoalveolar lavage

After animal euthanasia, the trachea was cannulated and secured using a silk suture. Cold PBS (500 mL) was delivered and retrieved through the cannula. The lavage was repeated 3 times. Bronchoalveolar lavage (BAL) fluid was used for virus titration.

Virus titration

BAL fluid viral titers were determined by standard plaque assay using Madin Darby canine kidney (MDCK) cells. Briefly, confluent monolayers of MDCK cells were infected with serially diluted BAL fluids. Infected monolayers were then covered with a semisolid overlay medium (Avicel). At 48 hours postinfection, cells were fixed using paraformaldehyde, and lysis plaques were counted after crystal violet counterstaining.

Histopathologic analysis and immunohistochemistry

Mouse lungs were fixed in 4% buffered ParaFormaldehye (PFA), were paraffin embedded, and then were cut into 4-μm sections. Lung sections were stained with hematoxylin-eosin-saffron and digitized using a slide scanner (Olympus VS120). A histopathologic analysis was performed by a pathologist using semiquantitative scoring for the following parameters: for destruction of the parenchyma the pathologist evaluated the architectural destruction of the lung; for peribronchial infiltrate, the pathologist evaluated the presence of inflammatory cells in the peribronchial area; for emphysema and alveolar septum rupture, the pathologist evaluated rupture of the partitions separating the alveoli with the formation of ''mega alveoli''; for thickening of the alveolar septum, the pathologist evaluated infiltration of the interalveolar partitions (thickening and/presence of inflammatory cells); for vascular congestion, the pathologist evaluated the presence of a large number of vessels filled with immune cells, regardless of their caliber; and for red

blood extravasation, the pathologist evaluated the presence of red blood cells outside the vascular lumens, either in the alveoli or in the supporting connective tissue.

Lung tissue dissociation

Human and mouse lung tissues were digested using the Tumor Dissociation Kit (Miltenyi Biotec) for 30 minutes at 37°C and 1500 rpm. The cells from the digested lung tissues were filtered using cell strainers (70 μm; Miltenyi Biotec) and were used for subsequent experiments.

Cell culture and irradiation procedure

After washing with PBS and centrifugation (300 g; 4°C; 5 minutes), the human lung cells were suspended and cultured in Dulbecco's Modified Eagle's Medium/Nutrient Mixture-F12 supplemented with both fetal bovine serum (FBS; 10%) and penicillin/streptomycin (1%). Human lung cells were incubated in the indicated medium at 37°C and in 5% CO2 for 30 minutes. Then, the adherent cells (macrophages and monocytes) were washed using PBS, and the nonadherent cells were discarded. The adherent cells were incubated in fresh medium (Dulbecco's Modified Eagle's Medium/ Nutrient Mixture-F12 containing 10% FBS and 1% penicillin/streptomycin) and stimulated with either Poly(I:C) at 1 ug/mL or PBS (for controls). At 6 hours after stimulation with the Poly(I:C), macrophages were irradiated using X-RAD320 (X-ray machine; 320 Kev, 4 mA) at a single dose of 0.5 or 1 Gy.

Flow cytometry

For cultured human lung macrophage staining, anti-CD169 (7-239) and anti-CD11c (REA618, Miltenyi Biotec) were used for membrane staining, while anti-IL-10 (REA842) and anti-IL-6 (REA1037, Miltenyi Biotec) were used for intracellular staining.

For mouse lung cell staining, cell suspensions were incubated with purified antimouse CD16/32 (clone 93, BioLegend) for 10 minutes at 4°C. For membrane staining, anti-Ly6G (REA526), anti-CD169 (REA197), anti-CD11c (REA754, Miltenyi Biotec), anti-CD11b (M1/70, BD HorizonTM), anti-Ly6C (HK 1.4), anti-D64 (X54-5/7.1, BioLegend), anti-SiglecF (E50-2440, BD HorizonTM), and anti-CD45 (REA737) antibodies were used to identify immune cells (CD45+), neutrophils (CD45+, Ly6G+), AMs (CD45+, CD11b-, CD64+, SiglecF+, CD11c+, CD169+), IMs (CD11b+ Ly6G- Ly6C-/low CD64+, CD11c+, CD169-), and NAMs (CD11b+ Ly6G- Ly6C-/low CD64+, CD11c-, CD169+). Anti−interferon (IFN)γ (XMG1.2, BD HorizonTM), anti-IL-6 (REA1034), and anti-IL-10 (REA1008) were used for intracellular staining. For membrane staining, cells were incubated with the antibody panel at the adapted

concentrations for 20 minutes at 4°C. Then, cells were fixed using 4% PFA for 15 minutes at 4°C and permeabilized for intracellular cytokine staining using Perm/Wash Buffer (BD Perm/WashTM). For intracellular staining, cells were preactivated before membrane staining using Cell Activation Cocktail (with Brefeldin A, Biolegend) for 2 hours at 37°C. Samples were acquired on an LSR Fortessa X20 (BD, Franklin Lakes, NJ) with FACSDiva software, and data were analyzed with FlowJo 10.0.7 software (Tree Star, Inc.).

Cytokine analysis

Cytokine concentrations in culture supernatants from in vitro−activated human macrophage samples were profiled. The proteins in the supernatant were diluted to 4 mg/mL and analyzed using MACSplex Human cytokine (Miltenyi Biotec), and data were analyzed with FlowLogic 7.3 software.

Statistical analysis

The statistical analysis was performed using GraphPad Prism 7. A 1-way analysis of variance was used to detect differences among multiple treatment groups. A P value $\leq$ .05 was considered significant. Data are expressed as means $\pm$ standard errors of means (SEMs).

Results

Low doses of RT protect mice from LPS-induced pneumonia and increase IL-10 production by NAMs

To investigate whether low doses of RT protect mice from lung inflammation, we treated mice with sublethal doses of LPS by intratracheal administration over 2 consecutive days. At 6 hours after the second intratracheal administration, mice were irradiated at the whole thorax at 0.5 or 1 Gy, and underwent CT imaging at the lung level at several time points after whole thorax irradiation. LPS administration significantly increased lung density at 96 hours (after administration of the first dose of LPS) compared with use of the PBS control, suggesting the development of an inflammatory process in the lungs (Fig. 1A). Interestingly, irradiated lungs at 1 Gy had a reduced lung density compared with those in the LPS group, suggesting that a low dose of 1 Gy protects mice from LPS-induced lung inflammation. Furthermore, a histopathologic analysis showed a decrease in parenchyma destruction (Fig. 1B) and a trend toward reduced peribronchial infiltration in irradiated lungs at 1 Gy (Fig. 1C).

NAMs act as main players to counteract lung inflammation via IL-10 secretion.[15] We therefore hypothesized that in the preclinical LPS pneumonia model, low doses of RT could stimulate IL-10 secretion by NAMs. Our results
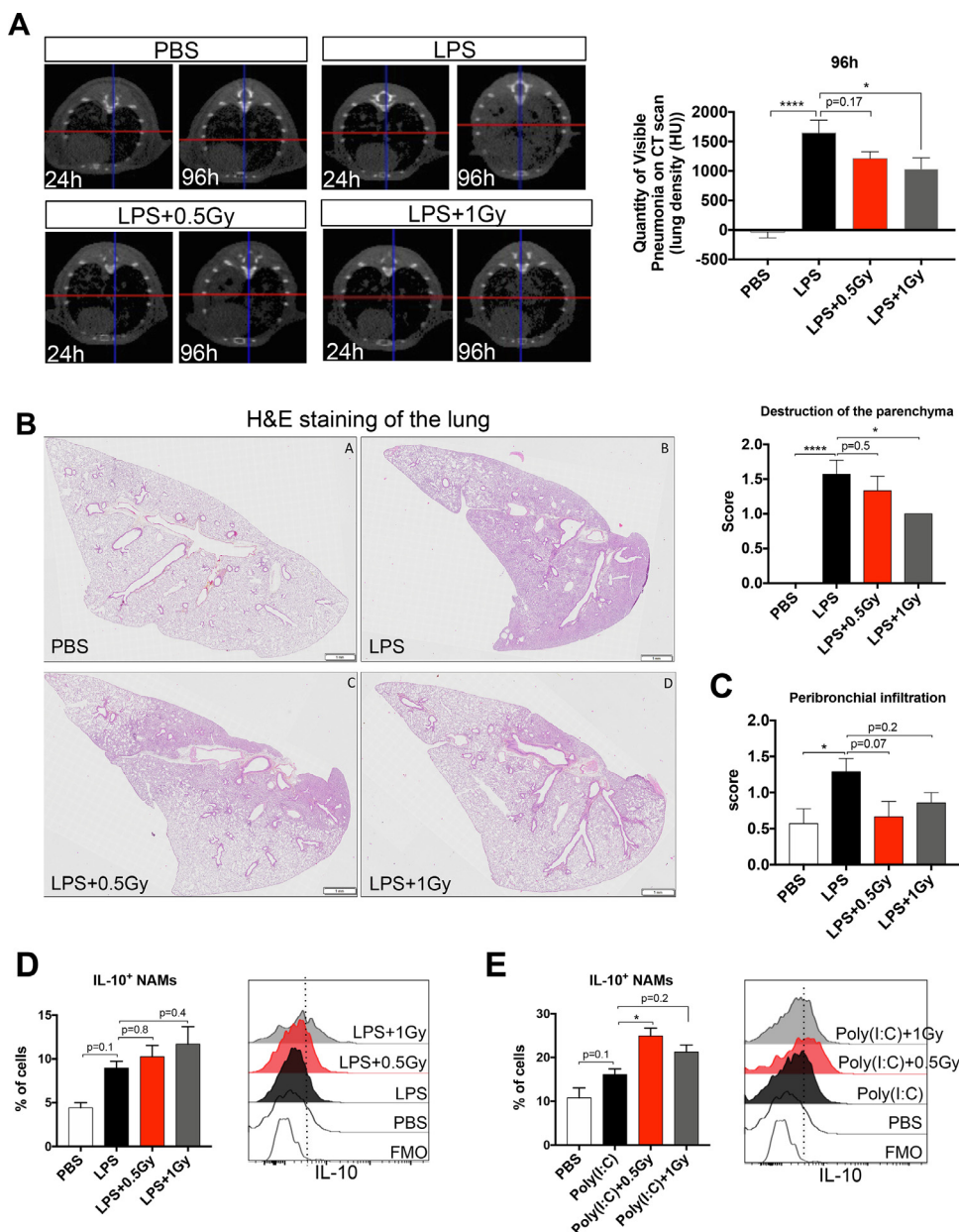
Fig. 1. Low doses of RT protect mice from LPS-induced pneumonia and increase IL-10 production by NAMs. Mice were treated with LPS or PBS by intratracheal administration for 2 consecutive days. At 6 hours after the second intratracheal administration, mice were irradiated at the whole thorax at 0.5 Gy or 1 Gy. (A) CT scans of lung density in different treatment groups 24 hours and 96 hours after the first dose of LPS (left) and lung density (HU) quantification in the different treatment groups 96 hours after the first dose of LPS (right). Data are from 3 independent experiments (n = 10-11). (B) Representative images (HES staining) of lungs from LPS-treated mice (left; scale bar = 1 mm) and scoring of the destruction of the parenchyma (right) 96 hours after the first dose of LPS. (C) Scoring of the peribronchial infiltrate. Data are representative of 2 independent experiments (n = 6-7). (D and E) At 18 hours after irradiation, the percentages of IL-10+ NAMs are presented for each treatment group (left), and representative histograms of the fluorescence associated with IL-10 in NAMs are shown for each treatment group (right). Data were obtained from 2 independent experiments (n = 7-8). For all data, bars indicate means and error bars indicate ±SEMs. *$P < .05$, ****$P < .0001$ (1-way ANOVA). *Abbreviations:* ANOVA = analysis of variance; CT = computed tomography; FMO = fluorescence minus one; Gy = Gray; H&E = hematoxylin and eosin; HES = hematoxylin-eosin-saffran; HU = Hounsfield Unit; IL = interleukin; LPS = lipopolysaccharide; NAM = nerve- and airway-associated macrophage; PBS = phosphate-buffered saline; RT = radiation therapy; SEM = standard error of the mean.

showed that LPS-induced lung inflammation is associated with a trend toward an increased percentage of NAMs producing IL-10 (Fig. 1D). Interestingly, low doses of RT further increased the percentage of NAMs producing IL-10 compared with the percentage in the nonirradiated group. Using a Poly(I:C)−induced inflammation model, we confirmed that low doses of RT induced greater increases in IL-10+ NAM percentages compared with those in PBS controls (Fig. 1E).

Low doses of RT decrease both histologic lung damage and immune cell infiltration during influenza virus infection

To evaluate the effect of low doses of RT on a viral pneumonia model, we treated mice with a lethal dose of PR8 virus (a murine-adapted influenza strain) by intranasal instillation. At 2 days after the instillation, mice were irradiated at the whole thorax at 0.5 or 1 Gy or/and treated with a single dose of dexamethasone. A histopathologic analysis of the lung showed that at 4 days after viral infection, the PR8 virus induced a significant increase in both emphysema/alveolar septum ruptures and thickening of the alveolar septum compared with the PBS group (Fig. 2A and B). Low doses of RT, as well as dexamethasone, decreased the emphysema/alveolar septum ruptures ($P = .0001$ for 0.5 Gy and $P = .06$ for both 1 Gy and dexamethasone), and a slight, even though nonsignificant, reduction of the thickening of the alveolar septum was observed with low doses of RT and dexamethasone groups compared with the PR8 condition. At 8 days postinfection, we observed significant increases in both vascular congestion and red blood cell extravasation in the PR8 group compared with the PBS group (Fig. 2C and D). Interestingly, low doses of RT or dexamethasone did not exacerbate vascular congestion and red blood cell extravasation compared with the PR8 group. More interestingly, low doses of RT and dexamethasone induced downward trends in both vascular congestion and red blood cell extravasation compared with the PR8 group.

The analysis of immune cell infiltrate in infected lungs 3 days postinfection showed that 0.5 Gy of RT induced a decreased number of CD45+ cells (Fig. 2E) and 1 Gy of RT or dexamethasone induced a trend toward a decreased number of CD45+ cells. The numbers of neutrophils, IMs, and NAMs significantly increased after PR8 infection, whereas they were not affected by the low doses of RT or dexamethasone (Fig. 2E). The number of IMs decreased after low doses of RT ($P = .07$ for 1 Gy) or dexamethasone treatment ($P < .05$). The number of AMs did not change regardless of the treatment. Low doses of RT combined with dexamethasone had the same effect as RT alone or dexamethasone alone on the immune cell infiltration, as the absolute number of immune cells was not affected by the RT and dexamethasone combination compared with either RT or dexamethasone alone (Fig. E1)A. Altogether, our data

show that low doses of RT aggravate neither tissue damage nor inflammatory cell infiltration in the lungs during viral infection.

Low doses of RT increase IL-10 production by lung immune cells during influenza virus infection

A flow cytometry analysis 3 days after PR8 infection showed that 0.5 Gy of RT, in contrast to dexamethasone treatment, induced a significant increase in the percent of NAMs producing IL- 10 (Fig. 3A). Low doses of RT combined with dexamethasone induced an upward trend in the percent of NAMs producing IL-10 compared with dexamethasone alone (Fig. E1B). The percent of NAMs producing both IFNγ and IL-6 significantly decreased in the PR8 group compared with the PBS group, and the NAM percentage was not affected by low doses of RT or dexamethasone (Fig. E2). Similarly, low doses of RT induced increases in the percentages of both AMs and neutrophils producing IL-10, compared with the other group (Fig. 3B and C). Low doses of RT combined with dexamethasone induced an increasing trend in the percentages of both AMs and neutrophils producing IL-10, compared with dexamethasone alone (Fig. E1B). The percentages of AMs and neutrophils producing IFNγ and IL-6 were not affected by the different treatments (Fig. E2). In agreement with data obtained with LPS and Poly(I:C) models, our data clearly show that low doses of RT during viral infection stimulate murine NAMs (as well as alveolar macrophages and neutrophils) to produce IL-10.

Low doses of RT increase IL-10 production and decrease IFNγ secretion by human lung macrophages in vitro

We then aimed to confirm whether low doses of RT could stimulate human lung macrophages to produce IL-10 (Fig. 4A). At 16 hours after human macrophage irradiation, culture supernatants were analyzed for cytokine secretion and human macrophage activation was analyzed by flow cytometry. The quantification of the supernatants showed that low doses of RT decreased IFNγ secretion and increased IL-10 secretion by Poly(I:C)-stimulated human lung macrophages compared with nonirradiated Poly(I:C)-stimulated ones (Fig. 4B). The levels of IFNγ, tumor necrosis factor (TNF) α, IL-2, and IL-9 were not affected by the low doses of RT.

Subsequently, we performed a flow cytometry analysis for human lung macrophages, and observed an increase in the percentage of human lung macrophages producing IL-10 after low-dose irradiation of 0.5 Gy compared with other culture conditions (Fig. 4C). Interestingly, the percentage of human lung macrophages producing IL-6 decreased after low-dose irradiation of 0.5 and 1 Gy compared with nonirradiated human lung macrophages (Fig. 4D).
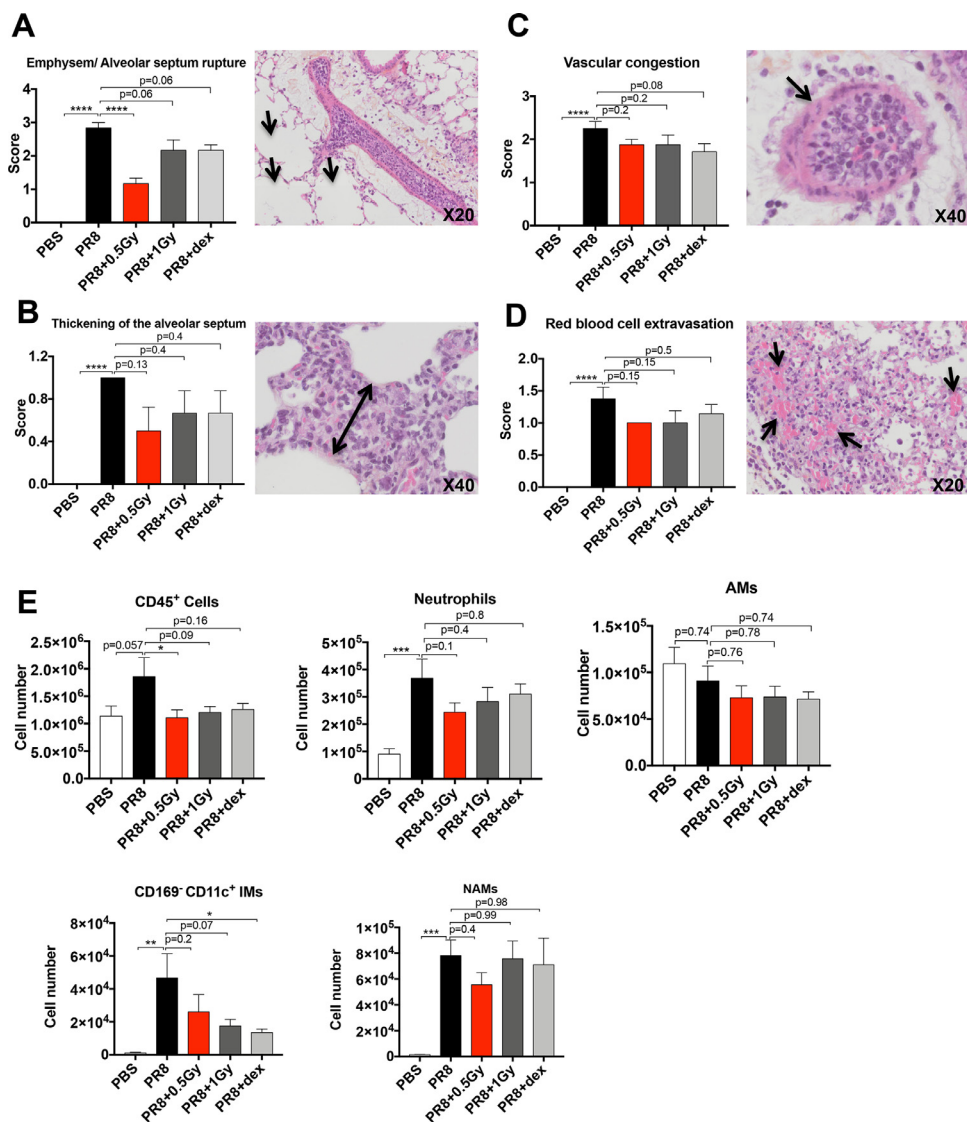
Fig. 2. Effect of low doses of RT on both lung tissue damages and immune cell infiltration in H1N1 pneumonia model. Mice were treated with PR8 influenza virus (H1N1) or PBS by intranasal instillation. After 2 days, mice were irradiated at the whole thorax at 0.5 Gy or 1 Gy or treated with dex. (A) Emphysem and alveolar septum rupture scoring 4 days after PR8 infection (left) and representative images (HES staining) of tissue lung from PR8-infected group (right). The arrows indicate emphysem. (B) Thickening of the alveolar septum scoring 4 days after PR8 infection (left) and representative images (HES staining) of tissue lung from the PR8-infected group (right). The double-pointed arrow indicates alveolar septum thickening. (C) Vascular congestion scoring in the lung tissue 8 days after PR8 infection (left) and representative images (HES staining) of tissue lung from the PR8-infected group (right). The arrow indicates vascular congestion. (D) Red blood cell extravasation scoring in the lung tissue 8 days after PR8 infection (left) and representative images (HES staining) of lung tissue from the PR8-infected group (right). The arrows indicate red blood cell extravasation. Data are from 2 independent experiments (n = 6-8). (E) Number of CD45+ cells, neutrophils, AMs, CD169- CD11c+ IMs, and NAMs in murine lungs 3 days after PR8 infection, analyzed by flow cytometry. Data are from 2 independent experiments (n = 6). For all data, bars indicate means and error bars indicate ±SEMs. *$P < .05$, **$P < .01$, ***$P < .001$, ****$P < .0001$ (1-way ANOVA). *Abbreviations:* AM = alveolar macrophage; ANOVA = analysis of variance; dex, dexamethasone; Gy = Gray; HES = hematoxylin-eosin-saffran; IM = interstitial macrophage; NAM = nerve- and airway-associated macrophage; PBS = phosphate-buffered saline; RT = radiation therapy; SEM = standard error of the mean.
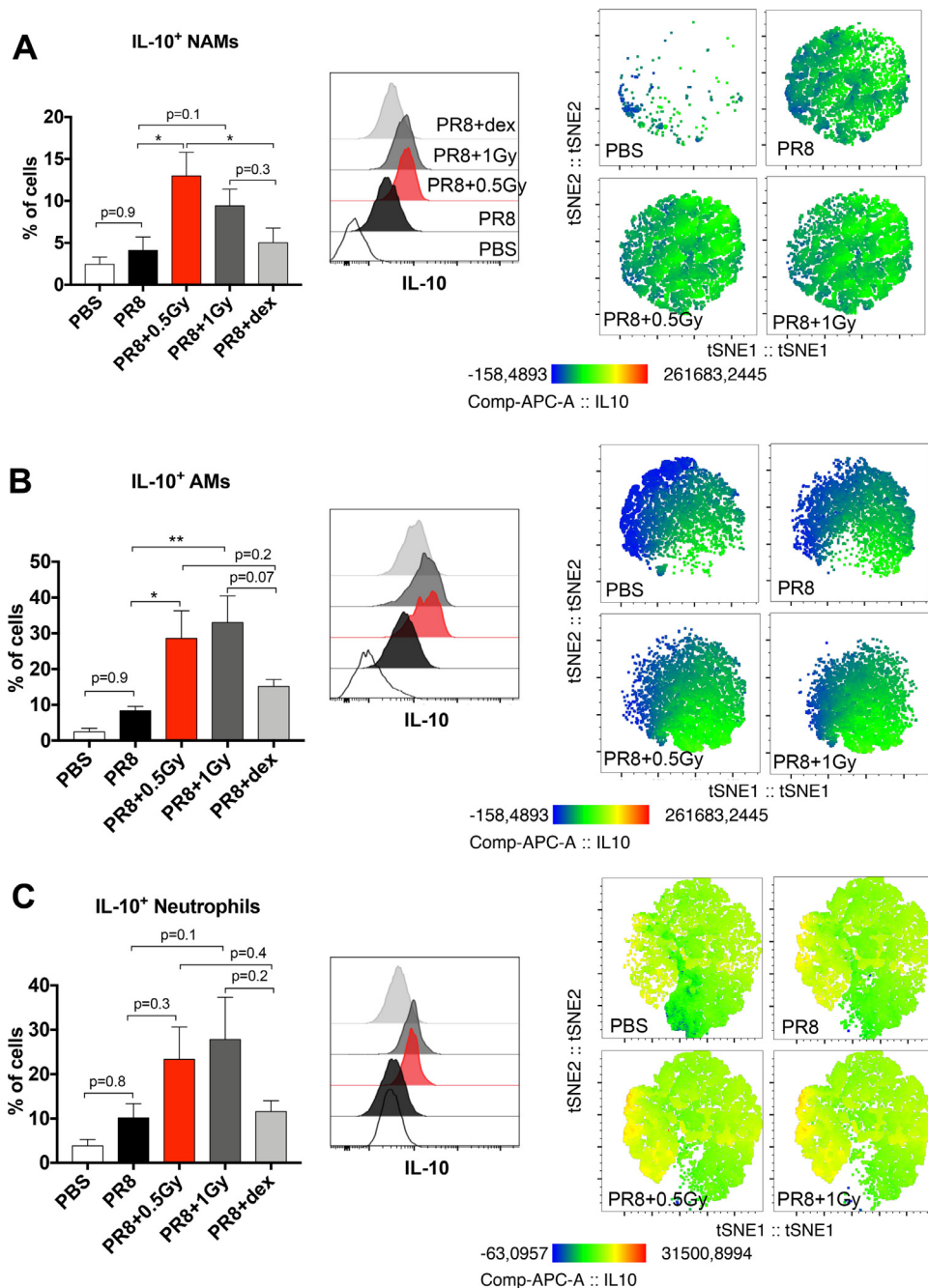
Fig. 3. Low doses of RT increase IL-10 production by immune cells in H1N1 pneumonia model. Mice were treated with PR8 influenza virus (H1N1) or PBS by intranasal instillation. After 2 days, mice were irradiated at the whole thorax at 0.5 Gy or 1 Gy or treated with dex. (A) At 3 days after PR8 infection, the percentages of IL-10+ NAMs are presented for each treatment group (left), and representative histograms of the mean fluorescence of IL-10 and t-SNE maps of IL10 expression in NAMs are shown (middle and right). (**B**) The percentages of IL-10+ AMs are presented for each treatment group (left), and representative histograms of the mean fluorescence of IL-10 and t-SNE maps of IL10 expression in AMs are shown (middle and right). (C) The percentages of IL-10+ neutrophils are presented for each treatment group (left), and representative histograms of the mean fluorescence of IL-10 and t-SNE maps of IL-10 expression in neutrophils are shown (middle and right). Data are from 2 independent experiments (n = 6). For all data, bars indicate means and error bars indicate ±SEMs. *P < .05, **P < .01 (1-way ANOVA). *Abbreviations:* AM = alveolar macrophage; ANOVA = analysis of variance; dex = dexamethasone; Gy = Gray; IL = interleukin; NAM = nerve- and airway-associated macrophage; PBS = phosphate-buffered saline; RT = radiation therapy; SEM = standard error of the mean; t-SNE = t-distributed stochastic neighbor embedding.
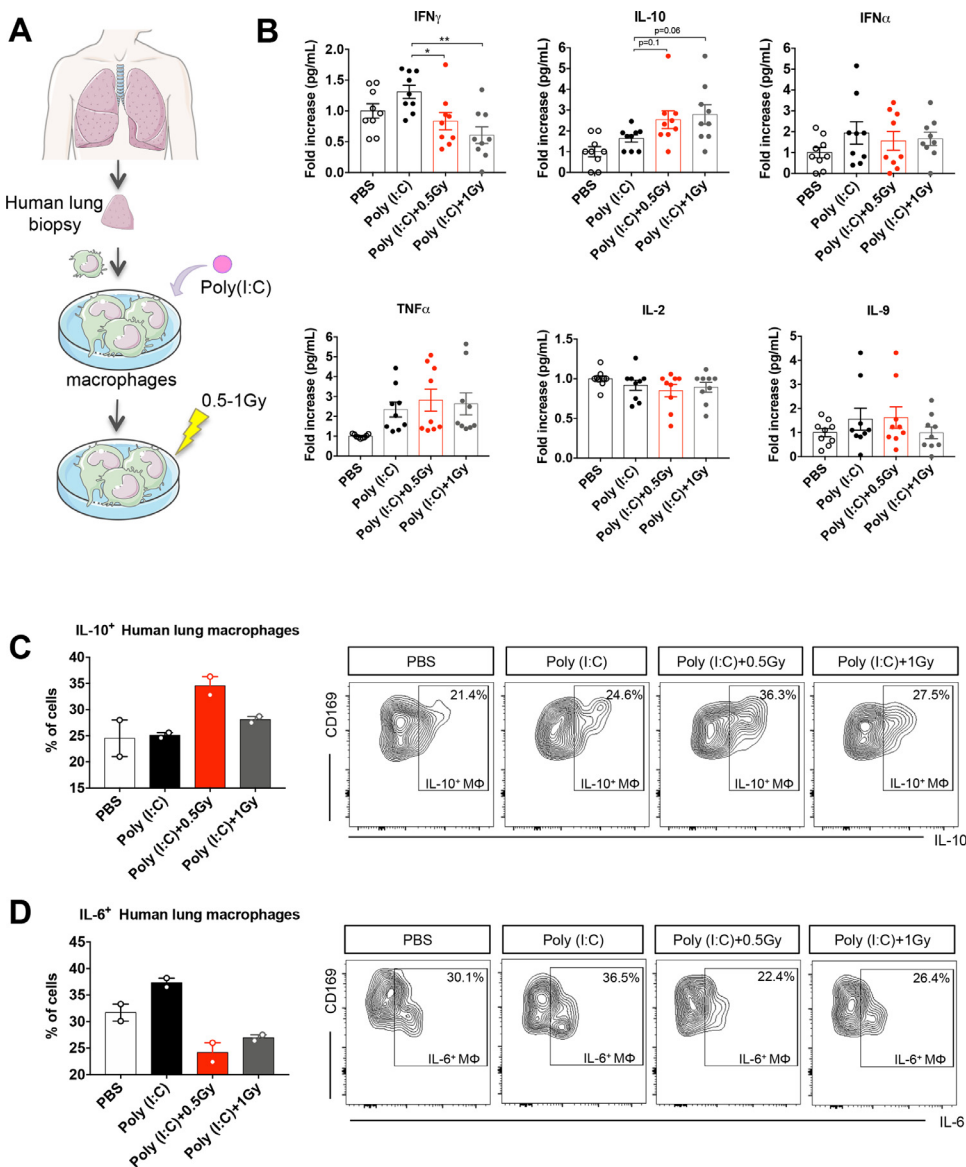
Fig. 4. Low doses of RT increase IL-10 production and decrease IFNγ secretion by human lung macrophages in vitro. (A) Human lung macrophages were stimulated in vitro using the TLR3 ligand Poly(I:C), or were treated with PBS (as control). After 6 hours, stimulated macrophages were irradiated at 0.5 Gy or 1 Gy. (B) At 16 hours after human macrophage irradiation, supernatants from cultured macrophages were analyzed for cytokine secretion. Data were obtained from 4 independent experiments (n = 9). (C) The percentages of IL-10+ human macrophages are presented for each treatment group (left) and gating strategy to identify human lung macrophages CD169+ producing IL-10 (right). (D) The percentages of IL-6 + human macrophages are presented for each treatment group (left) and gating strategy to identify human lung macrophages CD169+ producing IL-6 (right). For panels C and D, data were obtained from 1 experiment (n = 2). For all data, symbols and bars indicate means and error bars indicate ±SEMs. *P < .05, **P < .01 (1-way ANOVA). Data information: human lung macrophages were obtained from healthy lung biopsies. *Abbreviations:* ANOVA = analysis of variance; Gy = Gray; IFN = interferon; IL = interleukin; PBS = phosphate-buffered saline; Poly(I:C) = polyinosinic:polycytidylic acid; RT = radiation therapy; SEM = standard error of the mean; TLC = toll-like receptor; TNF = tumor necrosis factor.

Low doses of RT had no effect on H1N1 virus expansion in the lungs

Finally, we evaluated the impact of low doses of RT on the viral load in the lung. At 4 days after PR8 infection, broncho-alveolar lavage fluid samples from infected animals were analyzed for measurements of viral titers (Fig. 5A). Our results indicated that low doses of RT, as well as dexamethasone treatment, have no effect on virus levels in the lungs (Fig. 5B).
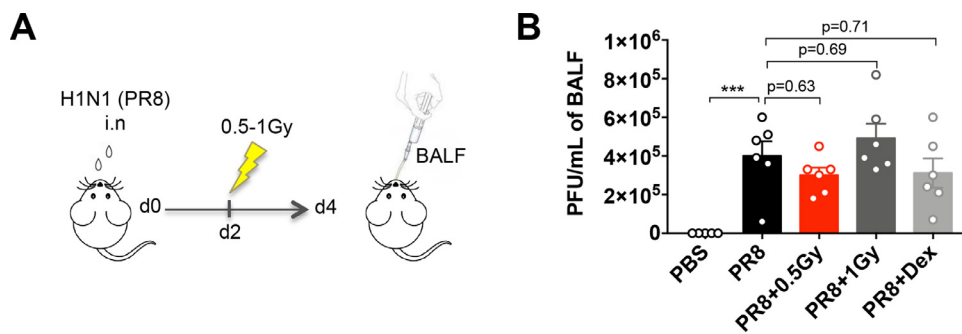
A

H1N1 (PR8)
i.n

0.5-1Gy

BALF

d0 ——————→ d4
      d2

B

Fig. 5. Low doses of RT have no effect on PR8 virus expansion. (A) Mice were treated with PR8 influenza virus (H1N1) or PBS by intranasal instillation. After 2 days, mice were irradiated at the whole thorax at 0.5 Gy or 1 Gy or treated with dex. (B) Virus titers were measured in the BAL 4 days after animal infection. Data were obtained from 2 independent experiments (n = 6). Symbols indicate means and error bars indicate ±SEMs. ***$P < .001$ (1-way ANOVA). *Abbreviations:* ANOVA = analysis of variance; BAL = bronchoalveolar lavage; BALF = broncho-alveolar lavage fluid; dex = dexamethasone; Gy = Gray; PBS = phosphate-buffered saline; PFU = plaque-forming unit; RT = radiation therapy; SEM = standard error of the mean.

Discussion

In the present study, we described the role of low doses of RT in (1) protecting mouse lungs from inflammation; (2) further stimulating the production of anti-inflammatory cytokine IL-10 by NAMs in vivo; and (3) counterbalancing the effect of the proinflammatory stimuli in vitro in human lung macrophages.

The effect of low doses of RT on the bone marrow−derived macrophage phenotype and on macrophage cell lines (RAW264.7 and THP-1) has already been reported elsewhere.

Interestingly, low doses of RT (0.5 Gy) affect the bone marrow−derived macrophage phenotype; however, this strongly depends on the microenvironment.[22] Furthermore, a decrease in IL-1b secretion by macrophage cell lines after low doses of RT (0.5 and 0.7 Gy) has been reported, and LPS-induced TNFα production was suppressed in 0.5 Gy−irradiated RAW264.7.[23,24] Accordingly, our results showed that human lung macrophages were affected by low doses of RT (0.5 and 1 Gy) in vitro. Irradiated human lung macrophages decreased IFNγ production and increased IL-10 secretion. Furthermore, the percentage of human lung macrophages producing IL-10 increased after low doses of RT, whereas the percentage of human lung macrophages producing IL-6 decreased after exposure to inflammatory stimuli. Our data demonstrate that low doses of RT are involved in limiting the inflammatory response in favor of an anti-inflammatory response. In preclinical pneumonia models, tissue-resident NAMs have been reported to robustly respond to inflammatory stimuli early during infection and to be the main negative regulators of inflammation in the lung, via IL-10 production as a potential mechanism.[15] Similarly, our data confirmed the production of IL-10 by NAMs after Poly(I:C), LPS and PR8 influenza virus infection. Furthermore, we observed that a low dose of RT protects mice from lung inflammation, does not

exacerbate lung tissue damages, and decreases immune cell infiltration. Whether or not the same NAMs that have been described in mice exist in human lungs with the same immunosuppressive function is not yet defined. Our data from in vitro−cultured human lung macrophages are not sufficient to answer this question, and further immuno-histological/cytofluorimetric analyses of human lung tissue are required.

In pneumonia, several old clinical studies have suggested improvement after low doses of RT.[5-7] However, after the onset of effective antimicrobial agents, the use of IR in the treatment of patients was discontinued, and the involved mechanism remained unknown. After the excess death toll related to the COVID-19 pandemic, some radiation oncologists suggested the use of low doses of RT to treat COVID-19 patients suffering from ARDS,[25-29] even if this raised some criticism[30-33] given the uncertainties regarding a potential viral flare-up or an increase in lung tissue damage.[34] In the absence of preclinical data, the scientific community is torn between the risks associated with whole-lung irradiation (acute worsening of the patients), and the immediate intrinsic risk of ARDS.[34] Our present study is the first to propose a key role for low doses of RT in the management of pneumonia using preclinical models, and suggests that lung macrophage reprogramming towards an immunosuppressive profile is one of the mechanisms involved.

Thrombotic events in the lungs of patients with COVID-19 after ARDS have been reported.[35] Our results show that PR8 influenza infection induces vessel congestion and obstruction, similar to what is observed in human COVID-19 lung infection. Interestingly, we show that low doses of RT do not worsen this phenomenon of obstructed vessels; on the contrary, there is a downward trend. Furthermore, AMs play a pivotal role in the antiviral defense during influenza virus pneumonia, and their depletion induced viral expansion.[15] Our results, obtained using a PR8 influenza pneumonia model, indicate that low doses of RT have no
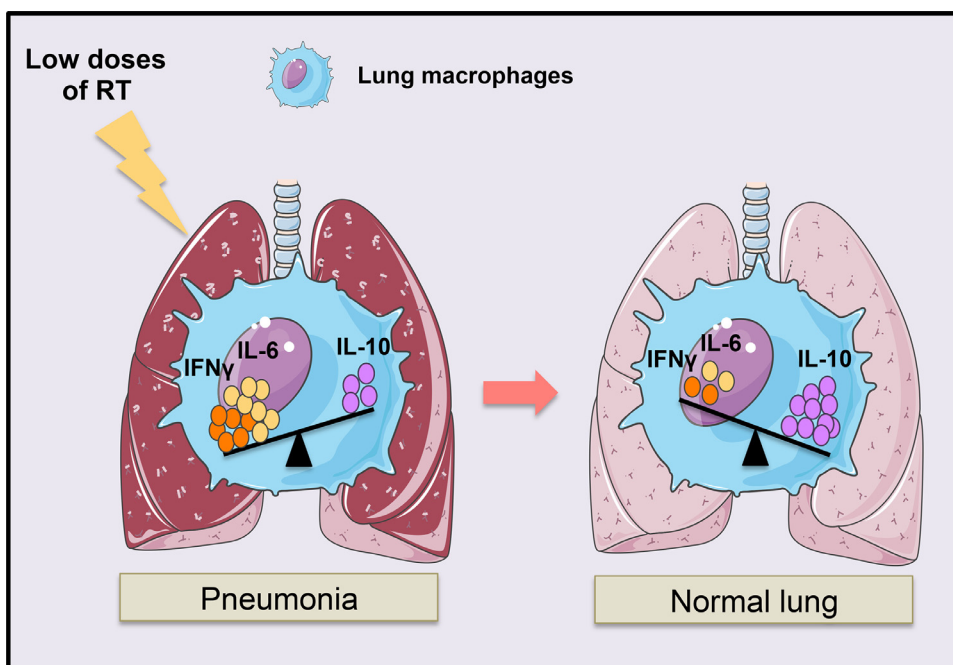
Fig. 6.   Lung macrophage reprogramming by low doses of RT during pneumonia. Low doses of RT induced the immunosuppressive profile of lung macrophages by increasing the IL- 10 production and decreasing the proinflammatory cytokines such as IFNγ leading to the lung inflammation resolution. *Abbreviations:* IFN = interferon; IL = interleukin; RT = radiation therapy.

effect on either the AM population or on viral expansion, suggesting that the use of low doses of RT would not negatively affect these parameters in viral pneumonias.

Our data show that low doses of RT decrease tissue damage in infected mice, and will contribute to define the optimal radiation dose to be used in the clinic. The optimal dose the minimum dose required to induce a maximal impact on macrophage reprogramming without tissue damage, and our data suggest that the 0.5-1 Gy range should be considered clinically. In line with our data, several clinical studies including pneumonia patients with advanced age or comorbidities presenting with COVID-19 reported an absence of acute toxicity after whole-thorax low doses of RT.[8,10]

In these clinical studies, the authors reported improvements in the respiratory functions of the patients in the hours after low doses of RT, with marked improvements on CT scans around 7 days after RT. These observations are in line with the kinetics of our observations. In summary, in line with the recent clinical data, the present study suggests that single, low-dose chest irradiation could be an efficient strategy to resolve human lung inflammation in pneumonia. Low doses of RT induce human lung macrophage reprogramming, in particular the production of the immunosuppressive IL-10 cytokine and the suppression of the inflammatory signals (IFNγ), which could be a mechanism by which low doses of RT protect from human pneumonia (Fig. 6). Interestingly, IFNγ− and TNFα−neutralizing treatments protect mice from both tissue damage and mortality during SARS-CoV-2 infection.[36]

Our study has several limitations, including the absence of the SARS-CoV-2 mouse model due to limited access to this model. Furthermore, due to difficulty accessing human

samples, we have not been able to collect healthy human lung tissue to repeat the experiment in Figure 4C and 4D. Our experiments were performed using only female mice, and it will be interesting to validate our data using male mice. Flow cytometry data showed that the RT plus dexamethasone combination induced a similar effect as that of RT alone in terms of the absolute number of infiltrating immune cells, and showed an upward trend in the production of the immunosuppressive IL-10 cytokine. These data do not seem to support a concomitant use of low doses of RT with dexamethasone to treat pneumonia. Nevertheless, clinical studies have been performed by treating COVID-19 patients whose clinical symptoms were progressing after dexamethasone treatment.[10] There is a need to conduct future preclinical studies evaluating sequential treatments of dexamethasone, followed by low doses of RT, to determine whether these treatments may be additive when separated over time. However, it is important to note that low doses of RT exerted effects of amplitude similar to, if not higher than, dexamethasone alone, suggesting that low doses of RT may be a therapeutic option, especially for patients not eligible for dexamethasone treatment.

Our data highlight the effects and good tolerance of low doses of RT on both human and murine macrophage reprogramming and the positive regulation of lung inflammation. Our findings are in agreement with the initial clinical data released from 2 out of the current 14 activated clinical trials worldwide evaluating chest RT for COVID-19 patients, and contribute to justifying the use of RT in this very unusual noncancer setting. Of note, the radiation doses used empirically in these clinical trials were not uniform; we do believe that carefully defining the lowest

possible effective dose is a major challenge at the heart of the current controversy, and our data underscore the fact that doses of 0.5-1 Gy are effective in reducing inflammation. These data provide a preclinical mechanistic support to clinical trials evaluating low doses of RT for COVID-19-induced ARDS.

References

1. Zhu N, Zhang D, Wang W, et al. China Novel Coronavirus Investigating and Research Team. A novel coronavirus from patients with pneumonia in China, 2019. *N Engl J Med* 2020;382:727–733.
2. Sheahan TP, Sims AC, Leist SR, et al. Comparative therapeutic efficacy of remdesivir and combination lopinavir, ritonavir, and interferon beta against MERS-CoV. *Nat Commun* 2020;11:222.
3. Mehta P, McAuley DF, Brown M, Sanchez E, Tattersall RS, Manson JJ. COVID-19: Consider cytokine storm syndromes and immunosuppression. *Lancet* 2020;395:1033–1034.
4. Silvin A, Chapuis N, Dunsmore G, et al. Elevated calprotectin and abnormal myeloid cell subsets discriminate severe from mild COVID-19. *Cell* 2020;182:1401–1418.e18.
5. Powell EV. Radiation therapy of lobar pneumonia. *Tex State J Med* 1936;32:237–240.
6. Oppenheimer A. Roentgen therapy of interstitial pneumonia. *J Pediatr* 1943;23:534–538.
7. Dubin IN, Baylin GJ, Gobble JW. The effect of roentgen therapy on experimental virus pneumonia; On pneumonia produced in white mice by swine influenza virus. *Am J Roentgenol Radium Ther* 1946;55:478–481.
8. Ameri A, Rahnama N, Bozorgmehr R, et al. Low-dose whole-lung irradiation for COVID-19 pneumonia: Short course results. *Int J Radiat Oncol Biol Phys* 2020;108:1134–1139.
9. Hess CB, Buchwald ZS, Stokes W, et al. Low-dose whole-lung radiation for COVID-19 pneumonia: Planned day 7 interim analysis of a registered clinical trial. *Cancer* 2020;126:5109–5113.
10. Hess CB, Nasti TH, Dhere V, et al. Immunomodulatory low-dose whole-lung radiation for patients with coronavirus disease 2019−Related pneumonia. *Int J Radiat Oncol Biol Phys* 2021;109:867–879.
11. Del Castillo R, Martinez D, Sarria GJ, et al. Low-dose radiotherapy for COVID-19 pneumonia treatment: Case report, procedure, and literature review. *Strahlenther Onkol Organ Dtsch Rontgengesellschaft Al* 2020;196:1086–1093.
12. Frey B, Rückert M, Deloch L, et al. Immunomodulation by ionizing radiation-impact for design of radio-immunotherapies and for treatment of inflammatory diseases. *Immunol Rev* 2017;280:231–248.
13. Davies LC, Jenkins SJ, Allen JE, Taylor PR. Tissue-resident macrophages. *Nat Immunol* 2013;14:986–995.
14. Chakarov S, Lim HY, Tan L, et al. Two distinct interstitial macrophage populations coexist across tissues in specific subtissular niches. *Science* 2019;363. eaau0964.
15. Ural BB, Yeung ST, Damani-Yokota P, et al. Identification of a nerve-associated, lung-resident interstitial macrophage subset with distinct localization and immunoregulatory properties. *Sci Immunol* 2020;5 eaax8756.
16. Merad M, Martin JC. Pathological inflammation in patients with COVID-19: A key role for monocytes and macrophages. *Nat Rev Immunol* 2020;20:355–362.
17. Meng Y, Beckett MA, Liang H, et al. Blockade of tumor necrosis factor alpha signaling in tumor-associated macrophages as a radiosensitizing strategy. *Cancer Res* 2010;70:1534–1543.
18. Rubin P, Finkelstein J, Shapiro D. Molecular biology mechanisms in the radiation induction of pulmonary injury syndromes: Interrelationship between the alveolar macrophage and the septal fibroblast. *Int J Radiat Oncol Biol Phys* 1992;24:93–101.
19. Klug F, Prakash H, Huber PE, et al. Low-dose irradiation programs macrophage differentiation to an iNOS⁺/M1 phenotype that orchestrates effective T cell immunotherapy. *Cancer Cell* 2013;24:589–602.
20. Meziani L, Mondini M, Petit B, et al. CSF1R inhibition prevents radiation pulmonary fibrosis by depletion of interstitial macrophages. *Eur Respir J* 2018;51 1702120.
21. Stowell NC, Seideman J, Raymond HA, et al. Long-term activation of TLR3 by Poly(I:C) induces inflammation and impairs lung function in mice. *Respir Res* 2009;10:43.
22. Deloch L, Fuchs J, Rückert M, Fietkau R, Frey B, Gaipl US. Low-dose irradiation differentially impacts macrophage phenotype in dependence of fibroblast-like synoviocytes and radiation dose. *J Immunol Res* 2019;3161750.
23. Conrad S, Ritter S, Fournier C, Nixdorff K. Differential effects of irradiation with carbon ions and X-rays on macrophage function. *J Radiat Res* 2009;50:223–231.
24. Lödermann B, Wunderlich R, Frey S, et al. Low dose ionising radiation leads to a NF-κB dependent decreased secretion of active IL-1β by activated macrophages with a discontinuous dose-dependency. *Int J Radiat Biol* 2012;88:727–734.
25. Kirkby C, Mackenzie M. Is low dose radiation therapy a potential treatment for COVID-19 pneumonia? *Radiother Oncol* 2020;147:221.
26. Lara PC, Nguyen NP, Macias-Verde D, et al. Whole-lung low dose irradiation for SARS-Cov2 induced pneumonia in the geriatric population: An old effective treatment for a new disease? Recommendation of the International Geriatric Radiotherapy Group. *Aging Dis* 2020;11:489–493.
27. Algara M, Arenas M, Marin J, et al. Low dose anti-inflammatory radiotherapy for the treatment of pneumonia by COVID-19: A proposal for a multi-centric prospective trial. *Clin Transl Radiat Oncol* 2020;24:29–33.
28. Cosset J-M, Deutsch É, Bazire L, Mazeron J-J, Chargari C. Low dose lung radiotherapy for COVID-19-related cytokine storm syndrome: Why not? *Cancer Radiother J Soc Francaise Radiother Oncol* 2020;24:179–181.
29. Dhawan G, Kapoor R, Dhawan R, et al. Low dose radiation therapy as a potential life saving treatment for COVID-19-induced acute respiratory distress syndrome (ARDS). *Radiother Oncol J Eur Soc Ther Radiol Oncol* 2020;147:212–216.
30. Kefayat A, Ghahremani F. Low dose radiation therapy for COVID-19 pneumonia: A double-edged sword. *Radiother Oncol J Eur Soc Ther Radiol Oncol* 2020;147:224–225.
31. Mortazavi SMJ, Kefayat A, Cai J. Low-dose radiation as a treatment for COVID-19 pneumonia: A threat or real opportunity? *Med. Phys.* 2020;47:3773–3776.
32. Magrini SM, Katz MS, Tomasini D, et al. Letter to the editor regarding "Lack of supporting data make the risks of a clinical trial of radiation therapy as a treatment for COVID-19 pneumonia unacceptable.". *Radiother Oncol J Eur Soc Ther Radiol Oncol* 2020;150:172–173.
33. Salomaa S, Bouffler SD, Atkinson MJ, Cardis E, Hamada N. Is there any supportive evidence for low dose radiotherapy for COVID-19 pneumonia? *Int J Radiat Biol* 2020;96:1228–1235.
34. Prasanna PG, Woloschak GE, DiCarlo AL, et al. Low-dose radiation therapy (LDRT) for COVID-19: Benefits or risks? *Radiat Res* 2020;194:452–464.
35. Ackermann M, Verleden SE, Kuehnel M, et al. Pulmonary vascular endothelialitis, thrombosis, and angiogenesis in COVID-19. *N Engl J Med* 2020;383:120–128.
36. Karki R, Sharma BR, Tuladhar S, et al. Synergism of TNF-α and IFN-γ triggers inflammatory cell death, tissue damage, and mortality in SARS-CoV-2 infection and cytokine shock syndromes. *Cell* 2021;184:149–168.e17.